

Article

Structures of Dimer-of-Dimers Type Defect Cubane Tetranuclear Copper(II) Complexes with Novel Dinucleating Ligands

Ryusei Hoshikawa ¹, Ryoji Mitsunashi ², Eiji Asato ³, Jianqiang Liu ⁴ and Hiroshi Sakiyama ^{1,*}
¹ Department of Science, Faculty of Science, Yamagata University, 1-4-12 Kojirakawa, Yamagata 990-8560, Japan; hosiryu@yahoo.com

² Institute of Liberal Arts and Science, Kanazawa University, Kakuma, Kanazawa, Ishikawa 920-1192, Japan; mitsunashi@staff.kanazawa-u.ac.jp

³ Department of Chemistry, Biology and Marine Science, Faculty of Science, University of the Ryukyus, Nishihara, Nakagami-gun, Okinawa 903-0213, Japan; asato@sci.u-ryukyu.ac.jp

⁴ Guangdong Provincial Key Laboratory of Research and Development of Natural Drugs, School of Pharmacy, Guangdong Medical University, Guangdong Medical University Key Laboratory of Research and Development of New Medical Materials, Dongguan 523808, China; jianqiangliu2010@126.com

* Correspondence: saki@sci.kj.yamagata-u.ac.jp

Abstract: Only a limited number of multinucleating ligands can stably maintain multinuclear metal structures in aqueous solutions. In this study, a water-soluble dinucleating ligand, 2,6-bis{[N-(carboxylatomethyl)-N-methyl-amino]methyl}-4-methylphenolate ((*sym*-cmp)³⁻), was prepared and its copper(II) complexes were structurally characterized. Using the single-crystal X-ray diffraction method, their dimer-of-dimers type defect cubane tetranuclear copper(II) structures were characterized for [Cu₄(*sym*-cmp)₂Cl₂(H₂O)₂] and [Cu₄(*sym*-cmp)₂(CH₃O)₂(CH₃OH)₂]. In the complexes, each copper(II) ion has a five-coordinate square-pyramidal coordination geometry. The coordination bond character was confirmed by the density functional theory (DFT) calculation on the basis of the crystal structure, whereby we found the bonding and anti-bonding molecular orbitals. From the cryomagnetic measurement and the magnetic analysis, overall antiferromagnetic interaction was observed, and this magnetic behavior is also explained by the DFT result. Judging from the molar conductance and the electronic spectra, the bridging chlorido ligand dissociates in water, but the dinuclear copper(II) structure was found to be maintained in an aqueous solution. In conclusion, the tetranuclear copper(II) structures were crystallographically characterized, and the dinuclear copper(II) structures were found to be stabilized even in an aqueous solution.

Keywords: tetranuclear copper(II) complex; dinucleating ligand; dimer-of-dimers type; crystal structure; magnetic properties; density functional theory (DFT)

Citation: Hoshikawa, R.; Mitsunashi, R.; Asato, E.; Liu, J.; Sakiyama, H. Structures of Dimer-of-Dimers Type Defect Cubane Tetranuclear Copper(II) Complexes with Novel Dinucleating Ligands. *Molecules* **2022**, *27*, 576. <https://doi.org/10.3390/molecules27020576>

Academic Editor:
Catherine Housecroft

Received: 24 December 2021

Accepted: 14 January 2022

Published: 17 January 2022

Publisher's Note: MDPI stays neutral with regard to jurisdictional claims in published maps and institutional affiliations.



Copyright: © 2022 by the authors. Licensee MDPI, Basel, Switzerland. This article is an open access article distributed under the terms and conditions of the Creative Commons Attribution (CC BY) license (<https://creativecommons.org/licenses/by/4.0/>).

1. Introduction

Copper is an essential trace element [1,2], and we humans cannot live without it. In fact, a 70 kg adult human body contains ~0.11 g of copper [1]. Humans need oxygen for cellular respiration to extract energy from food, and for cellular respiration, cytochrome *c* oxidase requires iron and copper to bind and activate oxygen [1–3]. In addition, toxic superoxide is produced daily together with cellular respiration, and superoxide dismutase (SOD) requires copper and zinc to decompose superoxide [1–3]. These are just a few examples of copper enzymes, and various copper proteins and copper enzymes play important roles in life. Some of the copper proteins have two or more copper ions at the active site and have functions that cannot be achieved by one copper ion. For the purpose of artificially realizing the function of such multi-copper proteins, many multinucleating ligands have been developed to stabilize the multinuclear metal complex structures.

2,6-Bis[bis(2-pyridylmethyl)aminomethyl]-4-methylphenol (H(bpmp)) is one of the most well-known acyclic dinucleating ligands, providing two N_3O coordination sites [4]. N,N' -(2-Hydroxy-5-methyl-1,3-xylylene)bis[N -(carboxymethyl)glycine] ($H_5(5\text{-Me-hxta})$) is another well-known acyclic dinucleating ligand, possessing two NO_3 coordination sites [5,6]. Both ligands, (bpmp) $^-$ and (5-Me-hxta) $^{5-}$, are end-off type acyclic dinucleating ligands with a phenolato moiety as a bridging group and are suitable for incorporating various dinuclear metal cores. In addition, metal complexes with these ligands and their derivatives [7] are stable in aqueous solutions, while Schiff base ligands are often hydrolyzed in aqueous solutions. When (bpmp) $^-$ or (5-Me-hxta) $^{5-}$ incorporates two octahedral metal ions, two coordination sites will be available for substrate incorporation in catalytic reactions. In this study, for the purpose of increasing the number of available coordination sites, a novel dinucleating ligand, 2,6-bis[[N -(carboxylatomethyl)- N -methyl-amino]methyl]-4-methylphenolate ((*sym-cmp*) $^{3-}$) was synthesized (Figure 1). The ligand (*sym-cmp*) $^{3-}$ has a bridging phenolato moiety and two NO_2 coordination sites and is expected to incorporate two metal ions. This paper reports the crystal structures of dimer-of-dimers type tetranuclear copper(II) complexes with (*sym-cmp*) $^{3-}$.

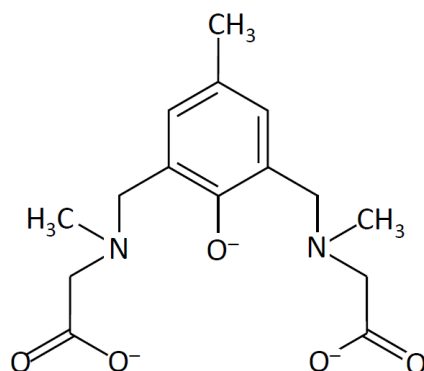


Figure 1. Chemical structure of (*sym-cmp*) $^{3-}$.

2. Results and Discussion

2.1. Preparation

2.1.1. Preparation of a Dinucleating Ligand

A dinucleating ligand, 2,6-bis[[N -(carboxylatomethyl)- N -methyl-amino]methyl]-4-methylphenolate ((*sym-cmp*) $^{3-}$) was synthesized via a Mannich reaction from *p*-cresol and sarcosine. The ligand was obtained as a sodium salt and recrystallized from ethanol. The ligand was characterized by IR, elemental analysis, 1H and ^{13}C NMR, and electrospray ionization (ESI) mass spectrometry. In 1H NMR, five singlet signals characteristic for (*sym-cmp*) $^{3-}$ were obtained (Figure S1), and in ^{13}C NMR, nine characteristic signals were obtained (Figure S2). In ESI-mass spectra, the main peak at $m/z = 309$ was assigned to [$H_2(sym-cmp)$] $^-$ (Figure S3), and its elemental composition ($C_{15}H_{21}N_2O_5$) was confirmed by the isotope pattern (Figure S4). Judging from the small molar conductance value ($19\text{ S}\cdot\text{cm}^2\cdot\text{mol}^{-1}$) in water, the sodium ions are considered to be tightly incorporated in the ligand.

2.1.2. Preparation of Copper(II) Complexes

With the dinucleating ligand (*sym-cmp*) $^{3-}$, tetranuclear copper(II) complexes were prepared as dimers of dinuclear copper(II) units. Using the copper(II) chloride, a chlorido complex, $[Cu_4(sym-cmp)_2Cl_2(H_2O)_2]\cdot 2H_2O$ (**1**), was obtained, while a methoxido derivative, $[Cu_4(sym-cmp)_2(CH_3O)_2(CH_3OH)_2]\cdot 2C_3H_7OH\cdot 2CH_3OH$ (**2**), was obtained by using the copper(II) nitrate. Purification of **2** was very difficult, and the crude product often contains nitrate ions. So, complex **2** was characterized only by the single-crystal X-ray diffraction method. Structural details will be described in the following crystallographic section (Section 2.2) and the theoretical calculation section (Section 2.4).

2.2. Crystal Structures of Copper(II) Complexes

2.2.1. Crystal Structures of $[\text{Cu}_4(\text{sym-cmp})_2\text{Cl}_2(\text{H}_2\text{O})_2] \cdot 2.4\text{CH}_3\text{OH} \cdot 1.8\text{H}_2\text{O}$ (**1'**)

Single crystals of **1'** were obtained by recrystallization of **1** from methanol. (Note that **1** is a dried sample, while **1'** is a sample in a crystalline state where drying was prevented.) Although **1** was considered to contain two water molecules as solvent of crystallization per tetranuclear copper(II) unit from the elemental analysis, solvents of crystallization of **1'** were empirically determined as 2.4 methanol and 1.8 water molecules. The crystal structure of the tetranuclear copper(II) complex $[\text{Cu}_4(\text{sym-cmp})_2\text{Cl}_2(\text{H}_2\text{O})_2]$ and its tetranuclear bridging structure are shown in Figure 2, and selected atomic distances and angles are summarized in Tables 1 and 2.

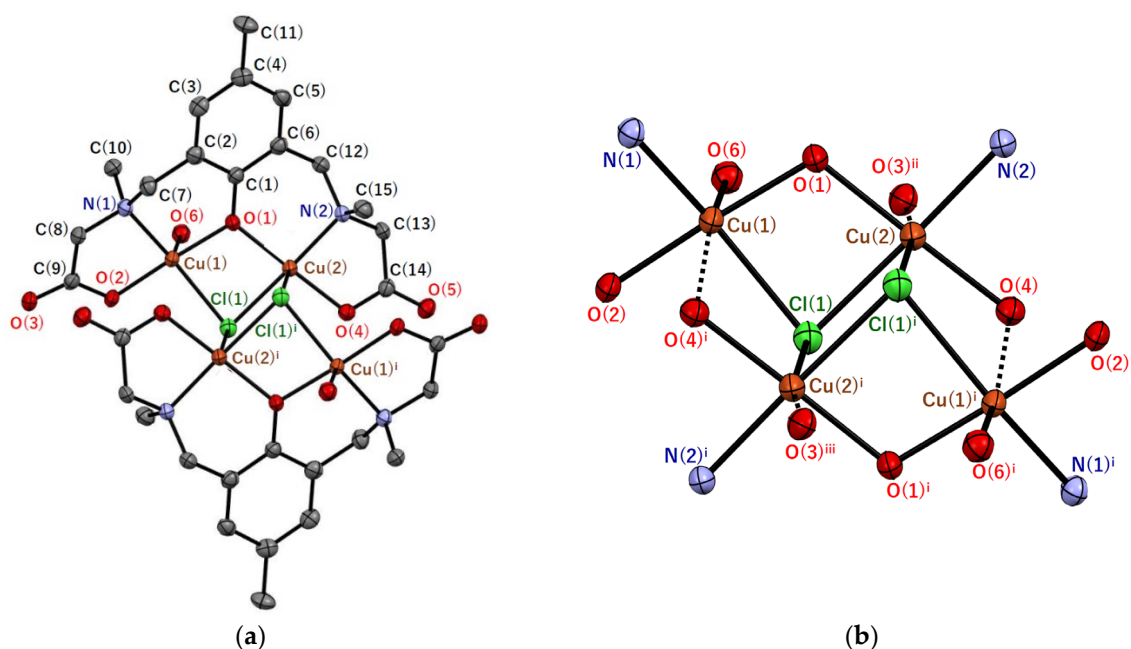


Figure 2. Molecular structures of (a) $[\text{Cu}_4(\text{sym-cmp})_2\text{Cl}_2(\text{H}_2\text{O})_2]$ and (b) $\text{Cu}_4\text{Cl}_2\text{N}_4\text{O}_{10}$ core in **1'** with atom labeling. Hydrogen atoms are omitted for clarity. Thermal ellipsoids are drawn at the 50% probability level. Symmetry code: ⁱ $(-x + 1/2, -y + 1/2, -z + 1)$, ⁱⁱ $(-x + 1/2, y + 1/2, -z + 3/2)$, ⁱⁱⁱ $(x, -y, z - 1/2)$.

Table 1. Selected distances for **1'**.

Atom–Atom ¹	Distance/Å	Atom–Atom ¹	Distance/Å
Cu(1)–Cl(1)	2.3638(14)	Cu(1)–O(1)	1.937(3)
Cu(1)–O(2)	1.926(3)	Cu(1)–O(6)	2.214(4)
Cu(1)–N(1)	1.998(4)	Cu(1)–O(4) ⁱ	3.208(4)
Cu(2)–Cl(1)	2.3113(14)	Cu(2)–O(1)	1.942(3)
Cu(2)–O(4)	1.936(3)	Cu(2)–N(2)	2.003(4)
Cu(2)–Cl(1) ⁱ	2.8012(14)	Cu(2)–O(3) ⁱⁱⁱ	2.804(4)
Cu(1)···Cu(2)	3.1274(8)	Cu(1)···Cu(1) ⁱ	5.8824(12)
Cu(1)···Cu(2) ⁱ	3.8024(9)	Cu(2)···Cu(2) ⁱ	3.7248(13)

¹ Symmetry code: ⁱ $(-x + 1/2, -y + 1/2, -z + 1)$, ⁱⁱ $(-x + 1/2, y + 1/2, -z + 3/2)$.

Table 2. Selected angles for **1**'.

Atom–Atom–Atom ¹	Angle/°	Atom–Atom–Atom ¹	Angle/°
Cl(1)–Cu(1)–O(1)	83.38(11)	Cl(1)–Cu(1)–O(2)	94.87(10)
Cl(1)–Cu(1)–O(6)	94.72(10)	Cl(1)–Cu(1)–N(1)	161.10(12)
Cl(1)–Cu(1)–O(4) ⁱ	77.29(7)	O(1)–Cu(1)–O(2)	173.59(15)
O(1)–Cu(1)–O(6)	90.83(14)	O(1)–Cu(1)–N(1)	94.06(15)
O(1)–Cu(1)–O(4) ⁱ	92.89(12)	O(2)–Cu(1)–O(6)	95.46(14)
O(2)–Cu(1)–N(1)	85.61(15)	O(2)–Cu(1)–O(4) ⁱ	80.71(12)
O(6)–Cu(1)–N(1)	104.06(15)	O(6)–Cu(1)–O(4) ⁱ	170.73(12)
N(1)–Cu(1)–O(4) ⁱ	84.16(13)	Cl(1)–Cu(2)–O(1)	84.68(11)
Cl(1)–Cu(2)–O(4)	95.38(11)	Cl(1)–Cu(2)–N(2)	172.22(13)
Cl(1)–Cu(2)–Cl(1) ⁱ	86.96(5)	Cl(1)–Cu(2)–O(3) ⁱⁱ	84.35(8)
O(1)–Cu(2)–O(4)	175.93(15)	O(1)–Cu(2)–N(2)	94.72(16)
O(1)–Cu(2)–Cl(1) ⁱ	89.05(11)	O(1) ⁱ –Cu(2)–O(3) ⁱⁱ	130.04(9)
O(4)–Cu(2)–N(2)	84.66(15)	O(4)–Cu(2)–Cl(1) ⁱ	95.02(11)
O(4)–Cu(2)–O(3) ⁱⁱ	88.47(12)	N(2)–Cu(2)–Cl(1) ⁱ	100.79(12)
N(2)–Cu(2)–O(3) ⁱⁱ	87.87(14)	Cl(1) ⁱ –Cu(2)–O(3) ⁱⁱ	170.91(8)
Cu(1)–Cl(1)–Cu(2)	83.96(5)	Cu(1)–O(1)–Cu(2)	107.46(17)
Cu(1)–Cl(1)–Cu(2) ⁱ	94.44(4)	Cu(2)–Cl(1)–Cu(2) ⁱ	93.04(5)

¹ Symmetry code: ⁱ (−*x* + 1/2, −*y* + 1/2, −*z* + 1), ⁱⁱ (−*x* + 1/2, *y* + 1/2, −*z* + 3/2).

The tetranuclear copper(II) complex [Cu₄(*sym*-cmp)₂Cl₂(H₂O)₂] is centrosymmetric (Figure 2a) and considered as a dimer-of-dimers type tetranuclear copper(II) complex, possessing the defect cubane tetranuclear copper(II) core (Figure 2b). Each dinucleating ligand, (*sym*-cmp)^{3−}, incorporates two copper(II) ions bridged by one phenolic oxygen of the dinucleating ligand and by one chlorido ligand. If we consider only the typical coordination bonds, each copper(II) ion has five-coordinate square-pyramidal coordination geometry, and Cu(1) and Cu(2) ions are surrounded by NO₃Cl and NO₂Cl₂ donor sets, respectively. The distortion parameter τ defined as $\tau = (\theta - \varphi)/60 \times 100\%$ is calculated as 20.9% for Cu(1) and 6.1% for Cu(2), where θ° and φ° are the largest and the second largest bond angles around each copper atom, respectively. The parameter τ is 100% if the coordination geometry is purely trigonal-bipyramidal, while τ is 0% if the geometry is purely square-pyramidal. Therefore, both coordination geometries are considered to be square-pyramidal. Each of the apical bond distances (Cu(1)–O(6) = 2.222(3) Å and Cu(2)–Cl(1)ⁱ = 2.8011(13) Å) is longer than the other basal Cu–O (1.925(3)–1.943(3) Å) and Cu–Cl (2.3124(13)–2.3630(12) Å) bond lengths, respectively. This can be explained by the Jahn–Teller effect [8], typical for the copper(II) complexes with *d*⁹ electronic configuration.

The apical Cu–Cl distance (Cu(2)–Cl(1)ⁱ = 2.8011(13) Å) may seem to be slightly too long for the coordination bond; however, the covalent bond character was confirmed by the density functional theory (DFT) calculation (Section 2.4). Therefore, the chlorido ligand is definitely bridging three copper(II) ions, forming the defect cubane tetranuclear copper(II) core structure. On the other hand, two more weak coordination bonds were found by DFT calculations (dashed bonds in Figure 2b). One is the Cu(1)–O(4)ⁱ bond (3.209(3) Å), and the other is the Cu(2)–O(3)ⁱⁱ bond (2.804(4) Å) between Cu(2) and an oxygen atom in a neighboring tetranuclear copper(II) complex. Here, the weak coordination bond refers to a bond with less covalency than the typical coordination bond, where the overlap of atomic orbitals involved in the bond is smaller. When the weak coordination bonds are also taken into account, the coordination geometries around the two copper(II) ions are both octahedral.

Tetranuclear copper(II) complexes with similar tetranuclear copper(II) cores are reported [9–11], and their magnetic properties were analyzed. In two of them, all three adjacent copper(II) pairs are doubly bridged [9,10], while in the rest of them, two of the adjacent copper(II) pairs are doubly-bridged ones, but one pair is singly-bridged [11]. In a

precise sense, this type of core structure is often called the stepped cubane, but in the case of **1'**, the core structure can be included in the defect cubane.

2.2.2. Crystal Structures of $[\text{Cu}_4(\text{sym-cmp})_2(\text{CH}_3\text{O})_2(\text{CH}_3\text{OH})_2] \cdot 2\text{C}_3\text{H}_7\text{OH} \cdot 2\text{CH}_3\text{OH}$ (**2**)

Single crystals of **2** were obtained by slow diffusion of 2-propanol to a methanolic solution of the crude product. The crystal structure of the tetranuclear copper(II) complex $[\text{Cu}_4(\text{sym-cmp})_2(\text{CH}_3\text{O})_2(\text{CH}_3\text{OH})_2]$ and its tetranuclear bridging structure are shown in Figure 3, and selected atomic distances and angles are summarized in Tables 3 and 4.

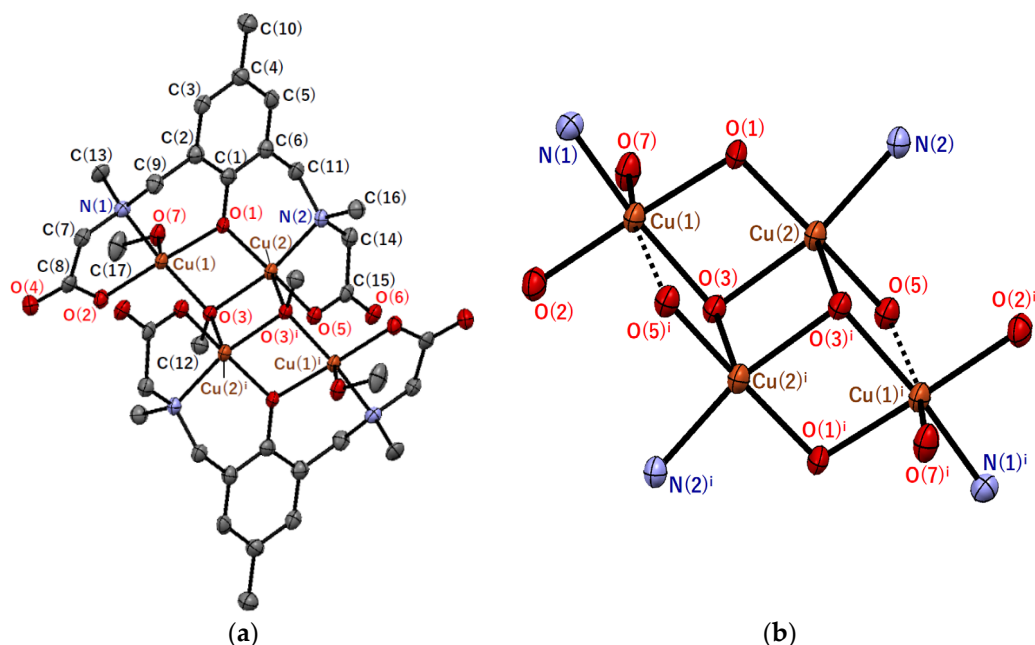


Figure 3. Molecular structures of (a) $[\text{Cu}_4(\text{sym-cmp})_2(\text{CH}_3\text{O})_2(\text{CH}_3\text{OH})_2]$ and (b) $\text{Cu}_4\text{N}_4\text{O}_{10}$ core in **2** with atom labeling. Hydrogen atoms are omitted for clarity. Thermal ellipsoids are drawn at the 50% probability level. Symmetry code: ⁱ $(-x + 1, -y + 1, -z + 1)$.

Table 3. Selected distances for **2**.

Atom–Atom ¹	Distance/Å	Atom–Atom ¹	Distance/Å
Cu(1)–O(1)	1.930(3)	Cu(1)–O(2)	1.933(3)
Cu(1)–O(3)	1.981(3)	Cu(1)–O(7)	2.331(3)
Cu(1)–N(1)	2.008(4)	Cu(1)–O(5) ⁱ	2.856(3)
Cu(2)–O(1)	1.930(3)	Cu(2)–O(3)	1.999(3)
Cu(2)–O(5)	1.936(3)	Cu(2)–N(2)	2.019(4)
Cu(2)–O(3) ⁱ	2.305(3)	Cu(2)···O(6) ⁱⁱ	3.3478(3)
Cu(1)···Cu(2)	3.0138(8)	Cu(1)···Cu(1) ⁱ	5.5123(12)
Cu(1)···Cu(2) ⁱ	3.3743(9)	Cu(2)···Cu(2) ⁱ	3.2483(11)

¹ Symmetry code: ⁱ $(-x + 1, -y + 1, -z + 1)$, ⁱⁱ $(-x + 2, -y + 1, -z + 1)$.

Table 4. Selected angles for **2**.

Atom–Atom–Atom ¹	Angle/°	Atom–Atom–Atom ¹	Angle/°
O(1)–Cu(1)–O(2)	174.14(13)	O(1)–Cu(1)–O(3)	79.22(13)
O(1)–Cu(1)–O(7)	88.52(13)	O(1)–Cu(1)–N(1)	93.40(14)
O(1)–Cu(1)–O(5) ⁱ	89.28(12)	O(2)–Cu(1)–O(3)	100.38(14)
O(2)–Cu(1)–O(7)	97.33(13)	O(2)–Cu(1)–N(1)	85.53(14)
O(2)–Cu(1)–O(5) ⁱ	84.96(11)	O(3)–Cu(1)–O(7)	90.78(13)
O(3)–Cu(1)–N(1)	164.26(14)	O(3)–Cu(1)–O(5) ⁱ	76.54(11)
O(7)–Cu(1)–N(1)	103.00(14)	O(7)–Cu(1)–O(5) ⁱ	167.32(11)
N(1)–Cu(1)–O(5) ⁱ	89.59(13)	O(1)–Cu(2)–O(3)	78.76(13)
O(1)–Cu(2)–O(5)	170.63(13)	O(1)–Cu(2)–N(2)	93.49(14)
O(1)–Cu(2)–O(3) ⁱ	96.27(13)	O(3)–Cu(2)–O(5)	99.19(13)
O(3)–Cu(2)–N(2)	164.05(15)	O(3)–Cu(2)–O(3) ⁱ	82.25(13)
O(5)–Cu(2)–N(2)	86.18(14)	O(5)–Cu(2)–O(3) ⁱ	92.48(12)
N(2)–Cu(2)–O(3) ⁱ	112.69(13)	Cu(1)–O(1)–Cu(2)	102.66(15)
Cu(1)–O(3)–Cu(2)	98.45(14)	Cu(1)–O(3)–Cu(2) ⁱ	103.63(13)
Cu(2)–O(3)–Cu(2) ⁱ	97.75(12)		

¹ Symmetry code: ⁱ (−*x* + 1, −*y* + 1, −*z* + 1).

The basic skeletal structure of the tetranuclear copper(II) complex [Cu₄(*sym*-cmp)₂(CH₃O)₂(CH₃OH)₂] in **2** is very similar to the complex structure in **1'**. That is, the bridging chlorido and water ligands in **1'** are replaced with methoxido and methanol ligands, respectively. The [Cu₄(*sym*-cmp)₂(CH₃O)₂(CH₃OH)₂] complex is centrosymmetric (Figure 3a) and considered a dimer-of-dimers type tetranuclear copper(II) complex, possessing the defect cubane tetranuclear copper(II) core (Figure 3b). A pair of copper(II) ions incorporated into one dinucleating ligand are bridged by one phenolic oxygen of the dinucleating ligand and by one methoxido ligand. Both types of copper(II) ions have five-coordinate square-pyramidal coordination geometries with NO₄ donor atoms, if we consider only the typical coordination bonds. The distortion parameter τ was 16.5% for Cu(1) and 11.0% for Cu(2). The apical bond distances (Cu(1)–O(7) = 2.331(3) Å and Cu(2)–O(3)ⁱ = 2.305(3) Å) are longer than the other basal Cu–O distances (1.930(3)–1.999(3) Å). The longer apical distances are consistent with the d⁹ electronic configuration of the copper(II) centers discussed in Section 2.2.1. When weak coordination bonds were also taken into account, another bond, Cu(1)–O(5)ⁱ (2.856(3) Å), was found in the DFT calculation, and the coordination geometry around Cu(1) became octahedral. In contrast, no covalent nature was observed between Cu(2) and adjacent O(6)ⁱⁱ in another complex.

2.3. Magnetic Properties

The cryomagnetic behavior for complex **1** was measured for the purpose of confirming the electronic configuration of the ground state and revealing the exchange interactions between the copper(II) ions. The $\chi_{\text{M}}T$ versus *T* plot is shown in Figure 4a. The observed $\chi_{\text{M}}T$ product at 300 K was 1.63 cm³·K·mol^{−1}, which was close to the spin-only value for the four independent *S* = 1/2 magnetic centers (1.50 cm³·K·mol^{−1}). The $\chi_{\text{M}}T$ value decreased on cooling to 1.9 K (0.026 cm³·K·mol^{−1}), suggesting a strong antiferromagnetic interaction between copper(II) ions. For the magnetic analysis, the method of Hatfield and Inman [12] was used to obtain the magnetic susceptibility equation. In this study, the Hamiltonian $\mathbf{H} = -J_1 (\mathbf{S}_{\text{A1}} \cdot \mathbf{S}_{\text{B1}} + \mathbf{S}_{\text{A2}} \cdot \mathbf{S}_{\text{B2}}) - J_2 \mathbf{S}_{\text{B1}} \cdot \mathbf{S}_{\text{B2}} - J_3 (\mathbf{S}_{\text{A1}} \cdot \mathbf{S}_{\text{B2}} + \mathbf{S}_{\text{A2}} \cdot \mathbf{S}_{\text{B1}}) - J_4 \mathbf{S}_{\text{A1}} \cdot \mathbf{S}_{\text{A2}}$ was used (see Figure 4b). The magnetic susceptibility equations (Equations (1)–(11)) used in this study are as follows:

$$\chi_M = \frac{Ng^2\beta^2}{kT} \frac{10 \exp(-\frac{A}{kT}) + 2 \exp(-\frac{B}{kT}) + 2 \exp(-\frac{C}{kT}) + 2 \exp(-\frac{D}{kT})}{5 \exp(-\frac{A}{kT}) + 3 \exp(-\frac{B}{kT}) + 3 \exp(-\frac{C}{kT}) + 3 \exp(-\frac{D}{kT}) + \exp(-\frac{E}{kT}) + \exp(-\frac{F}{kT})} (1 - \rho) + \frac{Ng^2\beta^2}{kT} \rho + 4 \text{ TIP}, \quad (1)$$

$$A = -\frac{K}{2} - Q, \quad (2)$$

$$B = -\frac{K}{2} + Q, \quad (3)$$

$$C = \frac{K}{2} - \sqrt{L^2 + P^2}, \quad (4)$$

$$D = \frac{K}{2} + \sqrt{L^2 + P^2}, \quad (5)$$

$$E = \frac{K}{2} + Q - \sqrt{K^2 + 3L^2 - 2KQ + Q^2}, \quad (6)$$

$$F = \frac{K}{2} + Q + \sqrt{K^2 + 3L^2 - 2KQ + Q^2}, \quad (7)$$

$$K = \frac{J_2 + J_4}{2}, \quad (8)$$

$$L = \frac{J_1 - J_3}{2}, \quad (9)$$

$$P = \frac{J_2 - J_4}{2}, \quad (10)$$

$$Q = \frac{J_1 + J_3}{2}, \quad (11)$$

where TIP and ρ are the temperature-independent paramagnetism per copper and the paramagnetic impurity with $S = 1/2$, respectively.

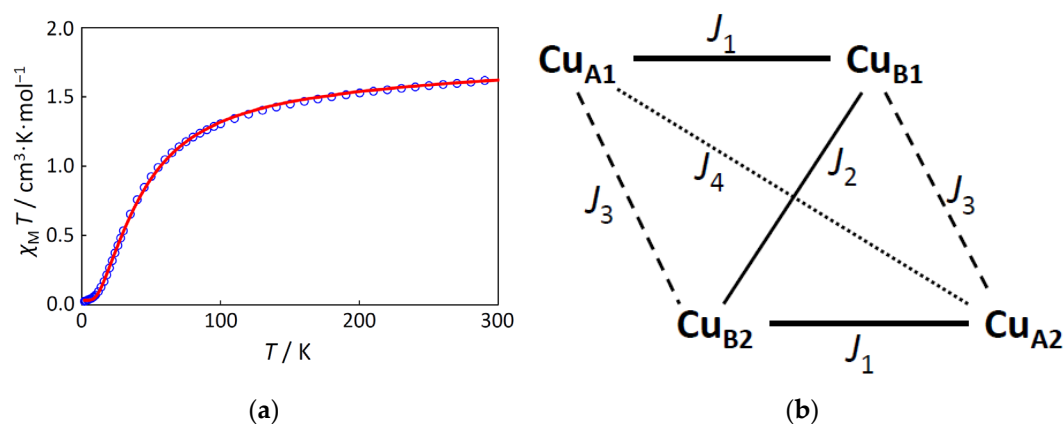


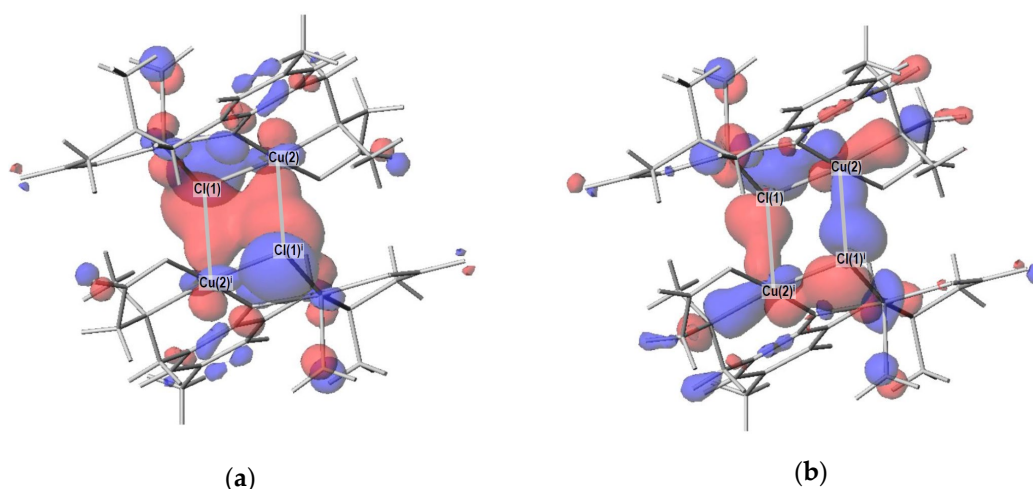
Figure 4. (a) The $\chi_M T$ versus T plot for **1**. The observed data (\circ) and the theoretical curve (—) with the best-fitting parameter set ($J_1, J_2, J_3, J_4, g, \text{TIP}, \rho$) = (−47.9 cm^{−1}, −38.5 cm^{−1}, 15.3 cm^{−1}, 0 cm^{−1} (fixed), 2.10, 60×10^{-6} cm³·mol^{−1} (fixed), 0.0196); (b) Interactions in the centrosymmetric tetranuclear copper(II) core.

As the result, the best fitting parameter set was found to be ($J_1, J_2, J_3, J_4, g, \text{TIP}, \rho$) = (−47.9 cm^{−1}, −38.5 cm^{−1}, 15.3 cm^{−1}, 0 cm^{−1} (fixed), 2.10, 60×10^{-6} cm³·mol^{−1} (fixed), 0.0196) with a good discrepancy factor ($R\chi = 7.2 \times 10^{-5}$). Overall, the magnetic interaction is

antiferromagnetic, but the strongest antiferromagnetic interaction is considered to occur between the copper(II) ions in the same dinucleating ligand, expressed as J_1 ($=-47.9\text{ cm}^{-1}$), bridged by one phenolato oxygen and one chlorido chlorine atoms. The second strongest antiferromagnetic interaction occurs between the copper(II) ions bridged by two chlorido ligands, expressed as J_2 ($=-38.5\text{ cm}^{-1}$). The third interaction, considered to be ferromagnetic, was between the copper(II) ions bridged by one chlorido ligand, expressed as J_3 ($=15.3\text{ cm}^{-1}$). This order, $|J_1| > |J_2| > |J_3|$, is consistent with the order of Cu...Cu distances. That is, the shorter the distance, the stronger the interaction, although this is a rough estimation. From the viewpoint of the molecular orbital theory, the magnetic orbitals should be on the basal planes of square-pyramidal coordination geometries around copper(II) ions. Using the local coordinates, each magnetic orbital is expressed as $d_{x^2-y^2}$, assuming the local z -axis to the apical direction and the local x - and y -axes to the donor atom directions in the basal plane. Since the two local magnetic orbitals of the pair of copper(II) ions in the same dinucleating ligand are almost in the same plane, the strongest antiferromagnetic interaction is expected between Cu_{A1} and Cu_{B1} in Figure 4b, expressed as J_1 . In this way, the obtained interaction parameters, J_1 , J_2 , and J_3 , can be reasonably understood. Other obtained parameters are also reasonable for copper(II) complexes.

2.4. Density Functional Theory (DFT) Calculation

In order to confirm the bonding nature around copper(II) ions in the complexes, density functional theory (DFT) calculations were conducted. In particular, the Cu(2)–Cl(1)ⁱ distance (2.8011(13) Å) in **1'** seems to be long, and whether this bond is a coordination bond or an ionic bond should be clarified based on the molecular orbital theory. As a result of the DFT calculation, bonding and anti-bonding orbitals were observed for the Cu(2)–Cl(1)ⁱ bond (Figure 5), indicating the covalent nature of the bond. Note that the coordination bond is the same as the covalent bond from the viewpoint of molecular orbital theory [13], although they were long considered to be different. In **1'**, the Cu(2)–Cl(1)ⁱ bond is formed using the d_{z^2} atomic orbital of Cu(2) atom and p_z atomic orbital of Cl(1)ⁱ, where the z direction is defined as the local apical direction around the Cu(2) atom. In this way, the five typical coordination bonds around each copper(II) ion were confirmed by the DFT calculations for both complexes **1'** and **2**. In addition, molecular orbitals with bonding and anti-bonding characters were found for each of the three weak coordination bonds (Cu(1)–O(4)ⁱ and Cu(2)–O(3)ⁱⁱ in **1'** and Cu(1)–O(5)ⁱ in **2**) discussed in Section 2.2, although the overlap of atomic orbitals involved was smaller than that of typical coordination bonds.



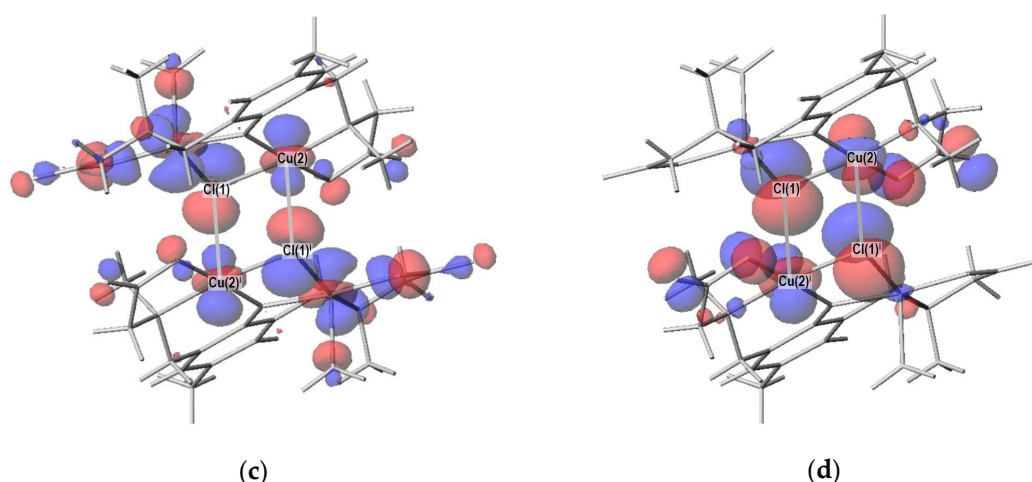


Figure 5. Molecular orbitals in **1'** with respect to the Cu(2)–Cl(1)ⁱ coordination bond: (a) *gerade* bonding orbital; (b) *ungerade* bonding orbital; (c) *gerade* anti-bonding orbital; (d) *ungerade* anti-bonding orbital.

Another purpose of the DFT calculation is to confirm the magnetic orbitals possessing the unpaired electrons. The doubly degenerate highest occupied molecular orbitals and doubly degenerate lowest unoccupied molecular orbitals were all found to be based on the local $d_{x^2-y^2}$ atomic orbitals of copper(II) ions orientated along the four donor atoms in the basal plane of each copper(II) coordination polyhedron. In addition, the strong antiferromagnetic interaction (J_1) between Cu(1) and Cu(2) was understood by the phenolato and chlorido bridges, considering the overlaps of the local magnetic orbitals and bridging atomic orbitals.

2.5. Electronic Spectra and Structure in Aqueous Solution

The electronic spectra of complex **1** were measured in water (Figure 6). Judging from the molar conductance in water (see Section 3.2), the chlorido ligands were thought to be dissociated in water to break the tetranuclear copper(II) structure. However, judging from the green color of the solution, copper(II) ions were thought to remain in the dinucleating ligand (*sym-cmp*)³⁻. The spectra are shown in Figure 6. The first band at around 15,000 cm⁻¹ can be assigned to the $d-d$ band. As a result of the Gaussian curve fitting, the first band was found to consist of two absorption components at around 14,200 cm⁻¹ and 16,400 cm⁻¹. The intensity of the first component is slightly larger than that of the second one, and this pattern is typical of trigonal-bipyramidal copper(II) complexes. Under the D_{3h} symmetry, the first and the second components are assigned to $^2A_{1'} \rightarrow ^2E'$ and $^2A_{1'} \rightarrow ^2E''$, respectively. The electronic spectra of the complexes containing trigonal-bipyramidal [CuCl₅]³⁻ anions were investigated earlier [14], and the positions of the components of **1** are found to be reasonable, considering the ligand-field strengths. This spectral feature of **1** suggests that all the copper(II) ions have almost the same structures, incorporated in the dinucleating ligand to form [Cu₂(*sym-cmp*)(H₂O)₄]⁺ species in aqueous solutions (Figure 7a). Generally, additional chlorido bridge or hydroxido bridge is expected to be formed between copper(II) ions; however, in this case, such an anionic bridging ligand is not so favorable because of the negative charge on the carboxylate side chains of the (*sym-cmp*)³⁻ ligand. This idea is consistent with the facile dissociation of the chlorido ligands in aqueous solutions confirmed by the conductivity measurement described previously.

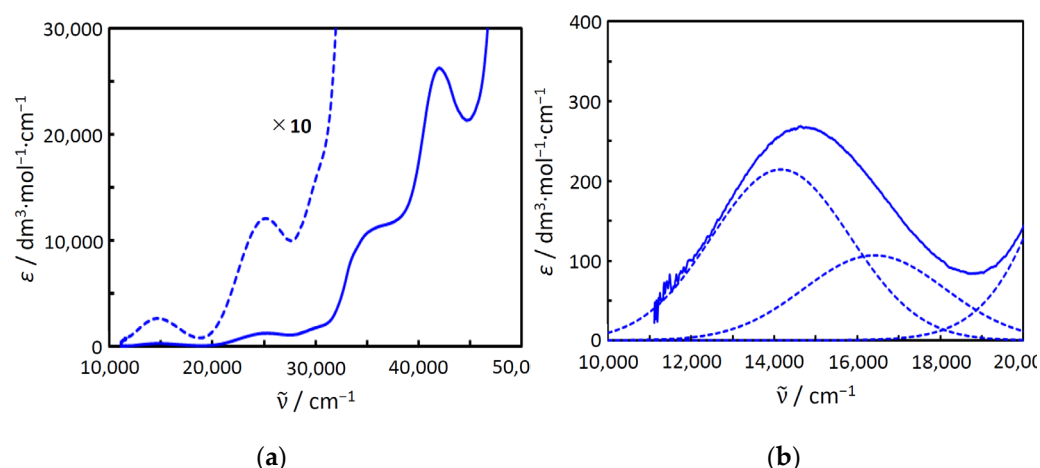


Figure 6. Electronic spectra of **1'** in water: (a) spectra in the range of 10,000–50,000 cm^{-1} ; (b) the first band with the Gaussian spectral components.

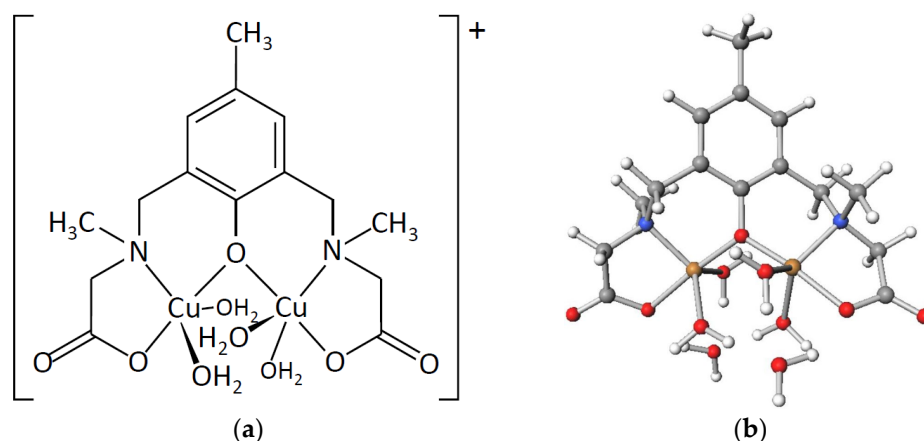


Figure 7. Proposed dinuclear copper(II) structure in aqueous solution: (a) chemical structure of $[\text{Cu}_2(\text{sym-cmp})(\text{H}_2\text{O})_4]^+$; (b) DFT-based optimized structure of $\{[\text{Cu}_2(\text{sym-cmp})(\text{H}_2\text{O})_4] \cdot 2\text{H}_2\text{O}\}^+$.

The proposed species in an aqueous solution, $[\text{Cu}_2(\text{sym-cmp})(\text{H}_2\text{O})_4]^+$, was confirmed on the basis of the DFT calculation assuming the water environment. Judging from the electronic spectra, the coordination geometry was trigonal-bipyramidal. When the $[\text{Cu}_2(\text{sym-cmp})(\text{H}_2\text{O})_4]^+$ was structurally optimized with two additional water molecules, the proposed trigonal-bipyramidal structure was successfully reproduced as shown in Figure 7b. The distortion parameter τ around the copper(II) ions fell in the range of 85.4–86.0%, which is considered to be trigonal-bipyramidal. This DFT result is strong evidence of the proposed structure. The proposed structure, including two copper(II) ions with four water molecules, is in concordance with the previously proposed structures for dinuclear cobalt(II) and nickel(II) complexes with a related dinucleating ligand in aqueous solutions [7].

2.6. Structures of Metal Complexes and Ligand Design

Similar to the popular (5-Me-hxta)⁵⁻ ligand, possessing four carboxylate chelating side chains, the (sym-cmp)³⁻ ligand in this study possesses two carboxylate chelating side chains. Although the number of side chains is reduced, the ligand is still capable of holding two copper(II) ions in an aqueous solution. With the reduction of the ligand-occupying sites, a larger substrate is expected to be incorporated at the coordination sites. On the other hand, changes in the ligand charge can lead to a variety of metal complex structures. For example, 2,6-bis[(2-hydroxyethyl)methylaminomethyl]-4-methylphenolate ((sym-hmp)⁻) [15] and 4-chloro-2,6-bis[(2-hydroxyethyl)methylaminomethyl] phenolate ((sym-

hcp)[−] [16] each have a skeletal structure very similar to (*sym*-cmp)^{3−} ligand; however, the obtained complex structures are different. The (*sym*-hmp)[−] and (*sym*-hcp)[−] ligands form 2:2 (ligand:metal) metal complexes, [M₂(*sym*-hmp)₂] (M = Mg(II) [17], Mn(II) [16], Co(II) [15,18,19], Ni(II) [20,21], Zn(II) [21]), while the (*sym*-cmp)^{3−} ligand forms 2:4 (ligand:metal) metal complexes, [M₄(*sym*-hmp)₂X₂Y₂] (M = Cu(II); X = Cl[−], CH₃O[−]; Y = H₂O, CH₃OH), as presented in this paper. This difference is thought to be caused by the difference in ligand charge. Concludingly, the skeletal structure, charge, bulkiness, etc., of the ligand can give rise to various metal complex structures. The knowledge of creating various controlled structures will also enable the development of metal-organic frameworks (MOFs) and is expected to be useful in various applications [22–29], beyond the use of molecular complexes as homogeneous catalysts.

3. Materials and Methods

3.1. Measurements

Elemental analyses (C, H, and N) were performed at the Elemental Analysis Service Centre of Kyushu University. Copper(II) ions were quantified by titration with ethylenediaminetetraacetic acid in the presence of hydrochloric acid, using murexide as an indicator. IR spectra were recorded on a Jasco FT/IR-4100 FT-IR spectrometer. ¹H and ¹³C NMR spectra (400 MHz) on a Bruker-Biospin AV 400 NMR spectrometer in D₂O, electrospray ionization (ESI) mass spectra on a Waters Quattro micro API mass spectrometer in methanol, and electronic spectra on Jasco V-560 (200–800 nm) and Hitachi 330 (800–2000 nm) spectrophotometers. Molar conductance was measured in H₂O on a DKK AOL-10 conductivity meter at room temperature. Magnetic susceptibility measurements were performed with a Quantum Design MPMS-7 SQUID magnetometer in the temperature range from 1.9 to 300 K with a static field of 5 kOe. The polycrystalline samples were ground into fine powders in an agate mortar. The sample was wrapped with aluminum foil. Data were corrected for paramagnetism of the aluminum foil. The susceptibilities were corrected for the diamagnetism of the samples by means of Pascal's constants.

3.2. Materials

All the chemicals were commercial products and were used as supplied. Methanol, ethanol, copper(II) nitrate–water (1/3), copper(II) chloride–water (1/2), paraformaldehyde, *p*-cresol, sodium hydroxide, lithium hydroxide–water (1/1), phosphorus pentoxide, 2-propanol, ethylenediaminetetraacetic acid, and hydrochloric acid were supplied by Nacalai Tesque Inc. (Kyoto, Japan). Sarcosine and murexide were supplied by Tokyo Chemical Industry Co., Ltd. (Tokyo, Japan).

3.3. Preparations

Disodium 2,6-bis[*N*-(carboxylatomethyl)-*N*-methyl-amino]methyl]-4-methylphenol–water (1/3) (Na₂H(*sym*-cmp)·3H₂O). To an aqueous solution (20 mL) containing *p*-cresol (5.41 g, 50 mmol), NaOH (6.10 g, 153 mmol), sarcosine (8.95 g, 100 mmol), and paraformaldehyde (3.00 g, 100 mmol) were added ethanol (20 mL) and the resulting solution was refluxed for 1 week. Ethanol and water were removed by evaporation to give Na₂H(*sym*-cmp) as a colorless powder. Yield 14.25 g (70%). (Found: C, 44.00; H, 6.45; N, 7.00; Calc. for C₁₅H₂₀N₂Na₂O₅·3H₂O: C, 44.10; H, 6.40; N, 6.85). Selected IR data [$\tilde{\nu}$ /cm^{−1}] using KBr disk (Figure S5): 3325, 2985, 2955, 2830, 1585, 1420, 1405, 1365, 1330, 1245, 855, 770, 715, 665. ¹H NMR in D₂O: δ 2.13 (s, 3 H), 2.27 (s, 6 H), 3.13 (s, 4 H), 3.67 (s, 4 H), 6.94 (s, 2 H). ¹³C NMR in D₂O: δ 19.29, 40.97, 56.74, 59.86, 122.77, 127.10, 130.81, 155.36, 177.46. ESI mass spectrum in MeOH: *m/z* 309, [H₂(*sym*-cmp)]⁺; 331, [NaH(*sym*-cmp)][−]. Molar conductance in H₂O [Λ /S·cm²·mol^{−1}] 19.

[Cu₄(*sym*-cmp)₂Cl₂(H₂O)₂]·2H₂O 1. To a methanolic solution (5 mL) of copper(II) chloride–water (1/2) (0.34 g, 2.0 mmol) was added a methanolic solution (5 mL) of Na₂H(*sym*-cmp)·3H₂O (0.38 g, 0.93 mmol), and the resulting solution was stirred for 30 min to give

the precipitation of green powder. Recrystallized from methanol, washed with methanol, and dried in vacuo over P_2O_5 . Yield 0.30 g (64%) (Found: C, 35.20; H, 4.60; N, 5.50; Cu, 24.70; Calc. for $C_{30}H_{42}Cl_2Cu_4N_4O_{12} \cdot 2H_2O$: C, 35.60; H, 4.60; N, 5.55; Cu, 25.10). Selected IR data [$\tilde{\nu}/cm^{-1}$] using KBr disk (Figure S6): 3050–3700, 3010, 2970, 2920, 2865, 2815, 1630, 1475, 1385, 1195, 870, 545, 465. Molar conductance in H_2O [$\Lambda/S \cdot cm^2 \cdot mol^{-1}$] 250 ($1.1 \times 10^{-3} mol \cdot dm^{-3}$), 250 ($5.7 \times 10^{-4} mol \cdot dm^{-3}$), 290 ($1.1 \times 10^{-4} mol \cdot dm^{-3}$).

$[Cu_4(sym-cmp)_2(CH_3O)_2(CH_3OH)_2] \cdot 2C_3H_7OH \cdot 2CH_3OH$ **2**. To a methanolic solution (5 mL) of copper(II) nitrate—water (1/3) (0.24 g, 0.99 mmol) was added a methanolic solution (5 mL) of $Na_2H(sym-cmp) \cdot 3H_2O$ (0.19 g, 0.47 mmol), and the resulting solution was refluxed for 2 h to give the precipitation of white powder. After filtration, the addition of 2-propanol (5 mL) resulted in the precipitation of dark-green powder. Recrystallized from methanol/2-propanol to give dark-green crystals. Yield 0.09 g (31%).

3.4. Crystallography

Crystallographic data are summarized in Table 5. Single crystals of **1'** suitable for X-ray analysis were obtained from a methanolic solution of **1**. Single crystals of **2** were obtained by slow diffusion of 2-propanol to a methanolic solution of the crude product. Single-crystal X-ray diffraction data were obtained with a Rigaku XtaLAB AFC11 diffractometer with graphite-monochromated Mo $K\alpha$ radiation ($\lambda = 0.71073 \text{ \AA}$). A single crystal was mounted with a glass capillary and flash-cooled with a cold N_2 gas stream. Data were processed using the CrysAlisPro software packages. The structure was solved by intrinsic phasing methods using the SHELXT [30] software packages and refined on F² (with all independent reflections) using the SHELXL [31] software packages. The non-hydrogen atoms were refined anisotropically, and hydrogen atoms were refined using the riding model. Complex **2** was refined as a two-component twin with only the non-overlapping reflections of component 1 and was refined using the hklf 5 routine with all reflections of component 1 (including the overlapping ones). The Cambridge Crystallographic Data Centre (CCDC) deposition numbers are included in Table 5.

Table 5. Crystallographic data and refinement parameters of **1'** and **2**.

Complex	1'	2
Empirical formula ¹	$C_{16.2}H_{27.6}ClCu_2N_2O_{8.1}$	$C_{21}H_{38}Cu_2N_2O_9$
Formula weight ¹	542.53	589.61
Crystal system	Monoclinic	triclinic
Space group	$C2/c$	$P\bar{1}$
$a/\text{\AA}$	27.0693(14)	8.5827(6)
$b/\text{\AA}$	13.2690(5)	13.0679(8)
$c/\text{\AA}$	13.1356(7)	13.2862(7)
$\alpha/^\circ$	90	115.021(6)
$\beta/^\circ$	100.422(5)	102.208(5)
$\gamma/^\circ$	90	115.021(6)
$V/\text{\AA}^3$	4640.2(4)	1263.54(15)
Z ¹	8	2
Crystal dimensions/mm	$0.070 \times 0.050 \times 0.030$	$0.130 \times 0.057 \times 0.038$
T/K	100	100
$\lambda/\text{\AA}$	0.71073	0.71073
$\rho_{calcd}/g \cdot cm^{-3}$	1.553	1.645
μ/mm^{-1}	1.990	1.734
$F(000)$	2229	616
$2\theta_{max}/^\circ$	55	55
No. of reflections measured	9520	16014
No. of independent reflections	9520 (Rint = 0.0623)	5771 (Rint = 0.0770)

Data/restraints/parameters	9520/3/296	5771/45/341
$R1^2$ [$I > 2.00 \sigma(I)$]	0.0575	0.0674
$wR2^3$ (all reflections)	0.1664	0.1635
Goodness of fit indicator	1.020	0.992
Highest peak, deepest hole/ $e \text{ \AA}^{-3}$	1.787, −0.647	1.669, −1.068
CCDC deposition number	2130618	2130619

¹ Based on dinuclear unit, ² $R1 = \sum ||Fo| - |Fc|| / \sum |Fo|$, ³ $wR2 = [\sum (w(Fo^2 - Fc^2)^2) / \sum w(Fo^2)^2]^{1/2}$.

3.5. Computation

Magnetic analyses and magnetic simulation were conducted using the MagSaki(TetraW9.2.0Cu) programs of the MagSaki series. DFT computations were performed using the GAMESS program [32,33] on Fujitsu PRIMERGY CX2550/CX2560 M4 (ITO super computer system) at Kyushu University. Calculations were performed with LC-BOP/6-31G [34]. When considering the solvent effect, the polarizable continuum model (PCM) method was used.

4. Conclusions

A water-soluble dinucleating ligand, (*sym*-cmp)^{3−}, was prepared, and two dimer-of-dimers type tetranuclear copper(II) complexes with (*sym*-cmp)^{3−} were prepared. The structures of the complexes were crystallographically characterized, and [Cu₄(*sym*-cmp)₂Cl₂(H₂O)₂] and [Cu₄(*sym*-cmp)₂(CH₃O)₂(CH₃OH)₂] complexes were found to have the defect cubane tetranuclear copper(II) core structures. In the complexes, each copper(II) ion has a five-coordinate square-pyramidal coordination geometry, and the coordination bonds were confirmed by the DFT calculation, whereby we found the bonding and anti-bonding molecular orbitals. The cryomagnetic measurement was conducted to find the overall antiferromagnetic interaction in the tetranuclear copper(II) structure. The observed magnetic data were successfully simulated with the tetranuclear model to find reasonable magnetic parameters. Judging from the molar conductance and the electronic spectra, the tetranuclear structure was found to be broken in an aqueous solution, but the dinuclear copper(II) structure, [Cu₂(*sym*-cmp)(H₂O)₄]⁺, was considered to be maintained in an aqueous solution. This proposed structure was supported by DFT calculation.

Supplementary Materials: The following supporting information can be downloaded. Figure S1: ¹H NMR of Na₂H(*sym*-cmp)·3H₂O, Figure S2: ¹³C NMR of Na₂H(*sym*-cmp)·3H₂O, Figure S3: ESI-mass spectra of Na₂H(*sym*-cmp)·3H₂O, Figure S4: Isotope pattern for Na₂H(*sym*-cmp)·3H₂O: (a) observed for *m/z* 309; (b) theoretical for *m/z* 309; (c) observed for *m/z* 331; (d) theoretical for *m/z* 331, Figure S5: IR spectra of Na₂H(*sym*-cmp)·3H₂O, Figure S6: IR spectra of **1**.

Author Contributions: Conceptualization, R.H. and H.S.; methodology, R.H., R.M., E.A. and H.S.; software, H.S.; validation, R.H. and H.S.; formal analysis, R.H., R.M., E.A. and H.S.; investigation, R.H., R.M., E.A. and H.S.; resources, R.H., R.M., J.L. and H.S.; data curation, R.H. and H.S.; writing—original draft preparation, R.H. and H.S.; writing—review and editing, R.H., R.M., E.A., J.L. and H.S.; visualization, R.H. and H.S.; supervision, H.S.; project administration, H.S. All authors have read and agreed to the published version of the manuscript.

Funding: This research received no external funding.

Institutional Review Board Statement: Not applicable.

Informed Consent Statement: Not applicable.

Data Availability Statement: The crystallographic data are available from the Cambridge Crystallographic Data Centre (CCDC). Other data not presented in Supplementary Materials are available on request from the corresponding author.

Acknowledgments: The magnetic measurements and the single-crystal X-ray measurement were conducted at the Institute of Molecular Science, supported by the Nanotechnology Platform Program (Molecule and Material Synthesis).

Conflicts of Interest: The authors declare no conflict of interest.

Sample Availability: Not applicable.

References

1. Kaim, W.; Schwederski, B. *Bioinorganic Chemistry: Inorganic Elements in the Chemistry of Life*; Wiley: Chichester, UK, 1991.
2. Cowan, J.A. *Inorganic Biochemistry*; VCH: New York, NY, USA, 1993.
3. Lippard, S.J.; Berg, J.M. *Principles of Bioinorganic Chemistry*; University Science Books: Mill Valley, CA, USA, 1994.
4. Suzuki, M.; Kanatomi, H.; Murase, I. Synthesis and properties of binuclear cobalt(II) oxygen adduct with 2,6-bis[bis(2-pyridylmethyl)aminomethyl]-4-methylphenol. *Chem. Lett.* **1981**, *10*, 1745–1748.
5. Murch, B.P.; Boyle, P.D.; Que, L., Jr. Structures of binuclear and tetranuclear iron(III) complexes as models for ferritin core formation. *J. Am. Chem. Soc.* **1985**, *107*, 6728–6729.
6. Murch, B.P.; Bradley, F.C.; Boyle, P.D.; Papaefthymiou, V.; Que, L.Jr. Iron-oxo aggregates. Crystal structures and solution characterization of 2-hydroxy-1,3-xylylenediaminetetraacetic acid complexes. *J. Am. Chem. Soc.* **1987**, *109*, 7993–8003.
7. Kazama, A.; Wada, A.; Sakiyama, H.; Hossain, M.J.; Nishida, Y. Synthesis of water-soluble dinuclear metal complexes [metal = cobalt(II) and nickel(II)] and their behavior in solution. *Inorg. Chim. Acta* **2008**, *361*, 2918–2922.
8. Jahn, H.A.; Teller, E. Stability of polyatomic molecules in degenerate electronic states I—Orbital degeneracy. *Proc. R. Soc. Lond. Ser. A-Math. Phys. Sci.* **1937**, *161*, 220–235.
9. Tandon, S.S.; Thompson, L.K.; Bridson, J.N.; Bubenik, M. Synthesis and structural and magnetic properties of mononuclear, dinuclear, and tetranuclear copper(II) complexes of a 17-membered macrocyclic ligand (HM3), capable of forming endogenous phenoxide and pyridazino bridges. X-ray crystal structures of $[\text{Cu}_2(\text{M3})(\mu_2\text{-OMe})(\text{NO}_3)_2]$, $[\text{Cu}_4(\text{M3})_2(\mu_3\text{-OMe})_2(\mu_2\text{-Cl})_2\text{Cl}_2]$, $[\text{Cu}_4(\text{M3})_2(\mu_3\text{-OEt})_2(\mu_2\text{-N}_3)_2(\text{N}_3)_2](\text{MeOH})$, $[\text{Cu}_4(\text{M3})_2(\mu_3\text{-OMe})_2(\text{NCS})_4](\text{DMF})$, and $[\text{Cu}(\text{M3})(\text{NCS})_2]$. *Inorg. Chem.* **1993**, *32*, 4621–4631.
10. Koikawa, M.; Yamashita, H.; Tokii, T. Crystal structures and magnetic properties of tetranuclear copper(II) complexes of N-(2-hydroxymethylphenyl)salicylideneimine with a defective double-cubane core. *Inorg. Chim. Acta* **2004**, *357*, 2635–2642.
11. Li, X.; Cheng, D.; Lin, J.; Li, Z.; Zheng, Y. Di-, tetra-, and hexanuclear hydroxy-bridged copper(II) cluster compounds: Syntheses, structures, and properties. *Cryst. Growth Des.* **2008**, *8*, 2853–2861.
12. Hatfield, W.E.; Inman, G.W. Spin-spin coupling in magnetically condensed complexes. IX. Exchange coupling constants for tetranuclear Schiff's base complexes of copper(II). *Inorg. Chem.* **1969**, *8*, 1376–1378.
13. The IUPAC Compendium of Chemical Terminology (Gold Book Version 2.3.3). Available online: <https://goldbook.iupac.org/> (accessed on 24 December 2021).
14. Allen, G.C.; Hush, N.S. Reflectance spectrum and electronic states of the CuCl_5^{3-} ion in a number of crystal lattices. *Inorg. Chem.* **1967**, *6*, 4–8.
15. Tone, K.; Sakiyama, H.; Mikuriya, M.; Yamasaki, M.; Nishida, Y. Magnetic behavior of dinuclear cobalt(II) complexes assumed to be caused by a paramagnetic impurity can be explained by tilts of local distortion axes. *Inorg. Chem. Commun.* **2007**, *10*, 944–947.
16. Sakiyama, H.; Kato, M.; Sasaki, S.; Tasaki, M.; Asato, E.; Koikawa, M. Synthesis and magnetic properties of a dinuclear manganese(II) complex with two manganese(II) ions of C_2 -twisted octahedral geometry. *Polyhedron* **2016**, *111*, 32–37.
17. Sakiyama, H.; Takahata, S.; Kashimoto, N.; Mitsuhashi, R.; Mikuriya, M. Crystal structure of a dinuclear magnesium(II) complex with 4-chloro-2,6-bis[(2-hydroxyethyl)methylaminomethyl]phenolate. *X-ray Struct. Anal. Online* **2017**, *33*, 75–76.
18. Deutsch, M.; Clauser, N.; Gillet, J.-M.; Lecomte, C.; Sakiyama, H.; Tone, K.; Souhassou, M. d-Orbital orientation in a dimer cobalt complex: Link to magnetic properties? *Acta Cryst.* **2011**, *B67*, 324–332.
19. Ridier, K.; Gillon, B.; Gukasov, A.; Chaboussant, G.; Cousson, A.; Luneau, D.; Borta, A.; Jacquot, J.-F.; Checa, R.; Chiba, Y.; et al. Polarized neutron diffraction as a tool for mapping molecular magnetic anisotropy: Local susceptibility tensors in Co^{II} complexes. *Chem. Eur. J.* **2016**, *22*, 724–735.
20. Sakiyama, H.; Tone, K.; Yamasaki, M.; Mikuriya, M. Electronic spectrum and magnetic properties of a dinuclear nickel(II) complex with two nickel(II) ions of C_2 -twisted octahedral geometry. *Inorg. Chim. Acta* **2011**, *365*, 183–189.
21. Sakiyama, H.; Chiba, Y.; Tone, K.; Yamasaki, M.; Mikuriya, M.; Krzystek, J.; Ozarowski, A. Magnetic properties of a dinuclear nickel(II) complex with 2,6-bis[(2-hydroxyethyl)methylaminomethyl]-4-methylphenolate. *Inorg. Chem.* **2017**, *56*, 138–146.
22. Pan, Y.; Rao, C.Y.; Tan, X.L.; Ling, Y.; Singh, A.; Kumar, A.; Li, B.H.; Liu, J.Q. Cobalt-seamed C-methylpyrogallol[4]arene nanocapsules-derived magnetic carbon cubes as advanced adsorbent toward drug contaminant removal. *Chem. Eng. J.* **2021**, 133857. <https://doi.org/10.1016/j.cej.2021.133857>.
23. Zhong, Y.Y.; Chen, C.; Liu, S.; Lu, C.Y.; Liu, D.; Pan, Y.; Sakiyama, H.; Muddassir, M.; Liu, J.Q. A new magnetic adsorbent of eggshell-zeolitic imidazolate framework for highly efficient removal of norfloxacin. *Dalton Trans.* **2021**, *50*, 18016–18026.
24. Sun, Y.M.; Jiang, X.D.; Liu, Y.W.; Liu, D.; Chen, C.; Lu, C.Y.; Zhuang, S.Z.; Kumar, A.; Liu, J.Q. Recent advances in $\text{Cu}(\text{II})/\text{Cu}(\text{I})$ -MOFs based nano-platforms for developing new nano-medicines. *J. Inorg. Biochem.* **2021**, *225*, 111599.
25. Liu, Y.W.; Zhou, L.Y.; Dong, Y.; Wang, R.; Pan, Y.; Zhuang, S.Z.; Liu, D.; Liu, J.Q. Recent developments on MOF-based platforms for antibacterial therapy. *RSC Med. Chem.* **2021**, *12*, 915–928.
26. Ding, Q.J.; Liu, Y.W.; Shi, C.C.; Xiao, J.F.; Dai, W.; Liu, D.; Chen, H.Y.; Li, B.H.; Liu, J.Q. Applications of ROS-Induced Zr-MOFs platform in multimodal synergistic therapy. *Mini-Rev. Med. Chem.* **2021**, *21*, 1718–1733.

27. Qiu, Y.Z.; Tan, G.J.; Fang, Y.Q.; Liu, S.; Zhou, Y.B.; Kumar, A.; Trivedi, M.; Liu, D.; Liu, J.Q. Biomedical applications of metal–organic framework (MOF)-based nano-enzymes. *New J. Chem.* **2021**, *45*, 20987–21000.
28. Wang, J.; Rao, C.Y.; Lu, L.; Zhang, S.L.; Muddassir, M.; Liu, J.Q. Efficient photocatalytic degradation of methyl violet using two new 3D MOFs directed by different carboxylate spacers. *Cryst. Eng. Comm.* **2021**, *23*, 741–747.
29. Liu, J.Q.; Luo, Z.D.; Pan, Y.; Singh, A.K.; Trivedi, M.; Kumar, A. Recent developments in luminescent coordination polymers: Designing strategies, sensing application and theoretical evidences. *Coord. Chem. Rev.* **2020**, *406*, 213145.
30. Sheldrick, G.M. A short history of SHELX. *Acta Cryst. Sect. A* **2008**, *64*, 112–122.
31. Sheldrick, G.M. Crystal structure refinement with SHELXL. *Acta Cryst. Sect. C* **2015**, *71*, 3–8.
32. Schmidt, M.W.; Baldrige, K.K.; Boatz, J.A.; Elbert, S.T.; Gordon, M.S.; Jensen, J.H.; Koseki, S.; Matsunaga, N.; Nguyen, K.A.; Su, S.; et al. General atomic and molecular electronic structure system. *J. Comput. Chem.* **1993**, *14*, 1347–1363.
33. Gordon, M.S.; Schmidt, M.W. *Advances in Electronic Structure Theory*; Elsevier: Amsterdam, The Netherlands, 2005.
34. Tawada, Y.; Tsuneda, T.; Yanagisawa, S.; Yanai, T.; Hirao, K. A long-range-corrected time-dependent density functional theory. *J. Chem. Phys.* **2004**, *120*, 8425–8433.